

CHAPTER 12. APPLICATIONS OF OPTICAL SENSING TO CROP HEALTH AND VIGOUR

James A. Taylor^{1,4}, Evangelos Anastasiou², Spyros Fountas², Bruno Tisseyre¹, Jose P. Molin³, Rodrigo G. Trevisan³, Hongyan Chen⁴ and Marcus Travers⁵

¹ITAP, Univ Montpellier, INRAE, Institut Agro, Montpellier, France; Case Study 12.2.

²Agricultural University of Athens, Athens, Greece; Case Study 12.1.

³USP, Piracicaba, SP, Brazil; Case Study 12.3.

⁴School of Natural and Environmental Sciences, University of Newcastle, Newcastle-upon-Tyne, UK; Case Study 12.4.

⁵Soil Essentials, Hilton of Fern, Brechin, Scotland, UK; Case Study 12.4.

Abstract

This chapter presents case studies that focus on canopy sensing using proximal and UAV-mounted optical sensors, rather than satellite-based optical sensing applications. The potential use of optical canopy sensing for crop quality and quantity is explored across four varied case studies. The case studies have been chosen to represent a diversity of crops, countries and stages of sensor development and translation (from emerging research to near commercial applications). In each case study, optical sensing is shown to be relevant to assessing productivity, either directly or through an indicator of crop health. It represents a powerful tool for crop management; however, across all the case studies, the optical sensing solution could only be used directly to address local issues. A clear message is that the suitability and adaptability of this technology to a variety of end-uses in cropping systems depends on local calibration and interpretation. The need for these is a limitation to technology adoption despite the widespread potential applications of optical sensors.

Keywords

Viticulture; Cotton; Potatoes; CropCircle; UAV; Vegetative indices; LiDAR; Ultrasonic sensors; multi-spectral; proximal sensors;

Introduction to the Chapter

This chapter presents four contrasting applications of crop sensors to various cropping systems including table grapes in Greece, wine-grapes in France, potato production in the United Kingdom and cotton production in Brazil. In each case, one or more canopy or crop sensors are used to assess crop vigour and to relate it to crop production, in terms of quantity and or quality. Collectively, they illustrate how information on plant vigour can be connected directly to production attributes or

can be used as an ancillary variable to assess another primary crop production attribute. They also illustrate a diversity of platforms (terrestrial, UAV and aerial) and a diversity of sensors (LiDAR, ultrasonic, optical infrared and optical visible) to obtain data on vigour. The case studies highlight the potential breadth of applications of crop vigour data, either directly or indirectly, in crop management, but this does not suggest that this is the full extent of potential uses. The case studies move from emerging research questions (such as the use of cumulative canopy reflectance responses over the season) to clear commercial applications (such as the incorporation of sensing into potato agronomy services).

A key message across the case studies is that sensor data help to identify spatial patterns in crop health and vigour, but also require local, site-specific interpretation and the ability to relate them directly to a production attribute and to a management operation. Ultimately this is the key objective when starting to collect spatio-temporal information on crop vigour.

The first case study describes a simple application of a proximal (tractor-mounted) visible–near-infrared (Vis–NIR) optical sensing system to table grapes. It explores the diversity of spectral data that can be derived from even simple multi-spectral systems and investigates which of the vegetative indices are the most useful for predicting table grape yield and quality. The second case study continues in the area of viticulture with a Vis–NIR optical sensor. However it focuses on wine grapes and on data obtained from an aerial platform. It does not directly relate the information on vigour to production attributes (as in case study 1), but rather uses the vigour data to identify and rank fields according to the amount of observed spatial variation in canopy vigour. This information is then used to sample intelligently for information related to vine water stress and to identify fields, and zones in fields, where crop vigour relates to vine water stress, and therefore to final grape quality.

Case study 3 concerns cotton production systems in Brazil. It compares optical sensors focused on crop vigour with sensors of crop height for mapping crop yield and productivity, especially at early developmental stages. Commercial optical sensing systems were robust and effective for spatial crop management. However, the alternative sensors were shown to work well in the given conditions. The LiDAR system, while experimental, was a particularly effective method of estimating crop biomass from crop height. The opportunities for sensor data-fusion and issues with sensor resolution versus input application resolution are discussed.

The final case study investigates potato production in the UK. This case study relies only on a simple RGB camera. It explores how cheap camera-based systems mounted on UAV platforms can give relevant and timely information on crop emergence and canopy development, even if the vigour of the canopy is not measured directly. Information on crop emergence and on canopy development, expressed as percentage ground cover, is used to update a local crop model. Scenarios run with the model in its native state and with the addition of different levels of information derived from the UAV images are used to demonstrate the value of basic colour images when used intelligently.

Case Study 12.1^a: Health and vigour for table grapes in Greece

Introduction

The world market for table grapes is large with production estimated at 27.3 million tonnes in 2018 (OIV, 2019). Farming practices and field conditions have a strong effect on the quantity and quality characteristics of table grapes. This is important because specific characteristics of table grapes will influence their commercial value. These quality characteristics are total soluble solids and berry diameter, as well as the berry sugar/acid ratio, which is strongly related with storability and consequently with shelf life (Sen et al. 2016; Tehrani et al. 2016). For this reason, high resolution vineyard information is desirable that relates to either or both the quantity or quality of berries in a field and can be used for management.

Proximal canopy sensing in vineyards is used to assess crop growth and yield variables in a non-destructive way and may include the use of radar, optical or multispectral sensors (Henry et al. 2019). The latter type of sensor (multispectral sensors) records information in different spectral bands that are being combined through mathematical equations for calculating the spectral vegetation indices (VIs) (Xue and Su, 2017). More specifically for vineyards, there are numerous VIs that have been used for assessing important crop variables such as vigour, yield and quality characteristics (e.g. total soluble solids and titratable acidity), as well as for pest and disease infestation and water stress (Hall et al. 2002; Tisseyre et al. 2007). The Normalized Difference Vegetation Index (NDVI) (Rouse et al. 1973) is the most common VI in agriculture (Badr et al. 2015). Although many studies have already found a significant relationship between a VI recorded at a single crop stage with vine vigour, yield and quality attributes, the studies do produce different degrees of correlation at different crop stages (Anastasiou et al. 2018). This has prompted the use of cumulative VIs that aggregate the values of the single crop stage VIs for providing better crop yield and quality assessments. The advantage of cumulative VIs is that the variable nature of the growing season is taken into account, resulting in a better correlation with crop yield and quality (Sun et al. 2017; Mirasi et al. 2019). However, there are no studies to date on the use of cumulative VIs in vineyards. Therefore the main aim of this case study was to assess the relationship between five different cumulative vegetation indices (VIs) and yield and quality attributes in a vineyard that had a large number of viticulture operations.

Materials and Methods

The study site was a commercial table grape vineyard (*Vitis vinifera* cv. Thompson seedless) near Athens, Greece with data collected over three consecutive years (2015-2017). Within the vineyard, there are two distinct soil texture types, a sandy clay loam and a clay loam. Each year the vineyard received approximately 2400

mm ha⁻¹ of water (irrigation + precipitation), 16 spray applications of foliar fertilizers, pesticides and crop growth regulators and 4 pruning operations to control the vine growth.

Canopy properties at six different developmental stages (fruit set [FS], pea-size berries [PS], majority of berries touching [BT], beginning of veraison [BV], middle of veraison [MV] and harvest [H]) were measured using a Crop Circle sensor (ACS-470, Holland Scientific Inc., Lincoln, NE, USA). The sensor was mounted at 1.5-m height above the soil surface and pointed horizontally at the vines from a distance of 1.2 m to scan the side ‘curtain’ (canopy) area of the vine. This particular canopy sensor has the ability to change filters and the wavelengths sensed according to user requirements. For the purposes of this experiment, six different filters with the same characteristics in terms of focal length were used, specifically, 532 nm (Green), 550 nm (Green), 670 nm (Red), 700 nm (Red-Edge), 730 nm (Red-Edge) and 760 nm (Near Infrared). The measurements were used for developing five VIs, the Normalized Difference Vegetation Index (NDVI), two versions of the Green Normalized Difference Vegetation Index (GNDVI) calculated with different wavelengths in the green region of the spectrum (550nm and 532 nm) and two versions of the Red-Edge Normalized Difference Vegetation Index (NDRE), using two different wavelengths (730 nm and 700 nm) in the Red-Edge area of the spectrum. Details of the formulae for the five VIs are given in Table 12.1. These VIs have previously shown good correlations with crop properties such as nitrogen uptake, biomass and leaf area index (LAI) in cereal crops (Rodriguez et al. 2006; Wang et al. 2007). Many researchers have proposed cumulative VIs for mapping and monitoring important crop variables such as net primary productivity, LAI, biomass and yield (Ricotta et al. 1999, Kross et al. 2015, Zhou et al. 2017).

Cumulative VIs were calculated by aggregating average VI values collected pre-veraison (FS, PS, BT), post-veraison (BV, MV, H) and at all stages (FS, PS, BT BV, MV, H) for each plot. This was done to assess the effect of the variation in vine vigour before and after veraison on correlations with final yield and quality characteristics.

For this study a regular grid of 36 cells (~10 × 25 m) was established across the vineyard to facilitate field sampling. This methodology follows the approach used by Tagarakis et al. (2013 and 2018). Samples of 50 berries were taken from each vineyard cell before harvest. Berry diameter was computed using image analysis in Image J (National Institutes of Health, USA). The berries were then crushed to produce juice using a juicing machine and the juice total soluble solids (TSS) (°Brix) measured by refractometry in an SR400 digital refractometer, the titratable acidity (TA) measured in a Fruit Acidity Meter GMK-708 (G-won Hitech Co., Seoul, South Korea) and the pH measured with an AD8000 multi-parameter meter (Adwa Hungary Kft., Szeged, Hungary). Harvest was performed manually on the 2–3 September 2015, the 21–22 August 2016 and the 16–17 August 2017. Table grape yield was estimated at harvest by measuring the number of bins per cell and multiplying it by the average bin weight.

Table 12.1. Formulae and references for the spectral vegetation indices (VIs) used in the current work.

Spectral Vegetation Index	Equation	References
NDVI	$NDVI = (\rho_{760} - \rho_{670}) / (\rho_{760} + \rho_{670})$	Rouse et al. 1974
GNDVI1	$GNDVI1 = (\rho_{760} - \rho_{550}) / (\rho_{760} + \rho_{550})$	Lymburner et al. 2000
GNDVI2	$GNDVI2 = (\rho_{760} - \rho_{532}) / (\rho_{760} + \rho_{532})$	Lymburner et al. 2000
NDRE1	$NDRE1 = (\rho_{760} - \rho_{730}) / (\rho_{760} + \rho_{730})$	Hunt et al. 2013
NDRE2	$NDRE2 = (\rho_{760} - \rho_{700}) / (\rho_{760} + \rho_{700})$	Hunt et al. 2013

Maps of yield and berry quality for the three years of study were produced using ArcGIS 10.2 software (ESRI Inc., Redlands, CA, USA). To assess the relationship between the cumulative VIs and table grape yield and quality, descriptive statistics, Pearson's correlation and regression analysis were performed. Step-wise linear regression was only performed for the cumulative VIs (cVI) that had the strongest correlation for each variable. The statistical analysis was performed with the statistical software Statgraphics 16 (StatPoint Technologies Inc., Warrenton, VA, USA).

Results and Discussion

There were variable weather conditions during the study. In this region the weather conditions from March to June are usually characterized by a considerable amount of precipitation and moderate temperatures, while July and August have higher temperatures and dry weather (Fig. 12.1). In 2016, however, precipitation was very limited and temperatures were higher during most crop stages. In contrast, in 2017 there was more precipitation that continued late into the growing season (July).

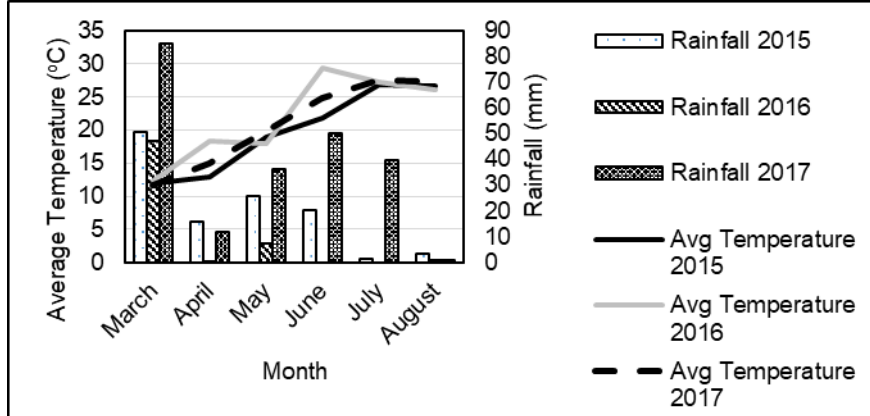


Figure 12.1 Monthly average temperature and precipitation from March to August of 2015, 2016 and 2017 table grape seasons.

The development of example VIs by crop stage and by year are shown in Fig. 12.2. The VIs showed more variation during pre-veraison crop stages than for post-veraison stages. This variation can be explained by the fact that weather conditions can greatly affect vine development and therefore yield (Cheng et al. 2014; Oczkowski, 2016; Ollat et al. 2016).

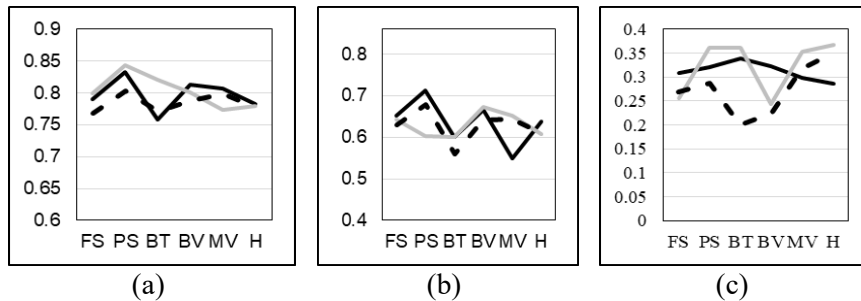


Figure 12.2 Temporal profiles of NDVI (a), GNDVI1 (b) and NDRE1 (c) averaged over the field at each sampling time (fruit set [FS], pea-size berries [PS], majority of berries touching [BT], beginning of veraison [BV], middle of veraison [MV] and harvest [H]) in three years (2015 – solid black; 2016 – solid grey; 2017 – dashed black line) These are shown as examples of the difference in response over time between the vegetation indices (VIs).

There was spatial variation of yield attributes between the different years (Fig. 12.3). Specifically, the south and east part of the field had the smallest values in terms of yield, berry diameter and titratable acidity for the three years of the study

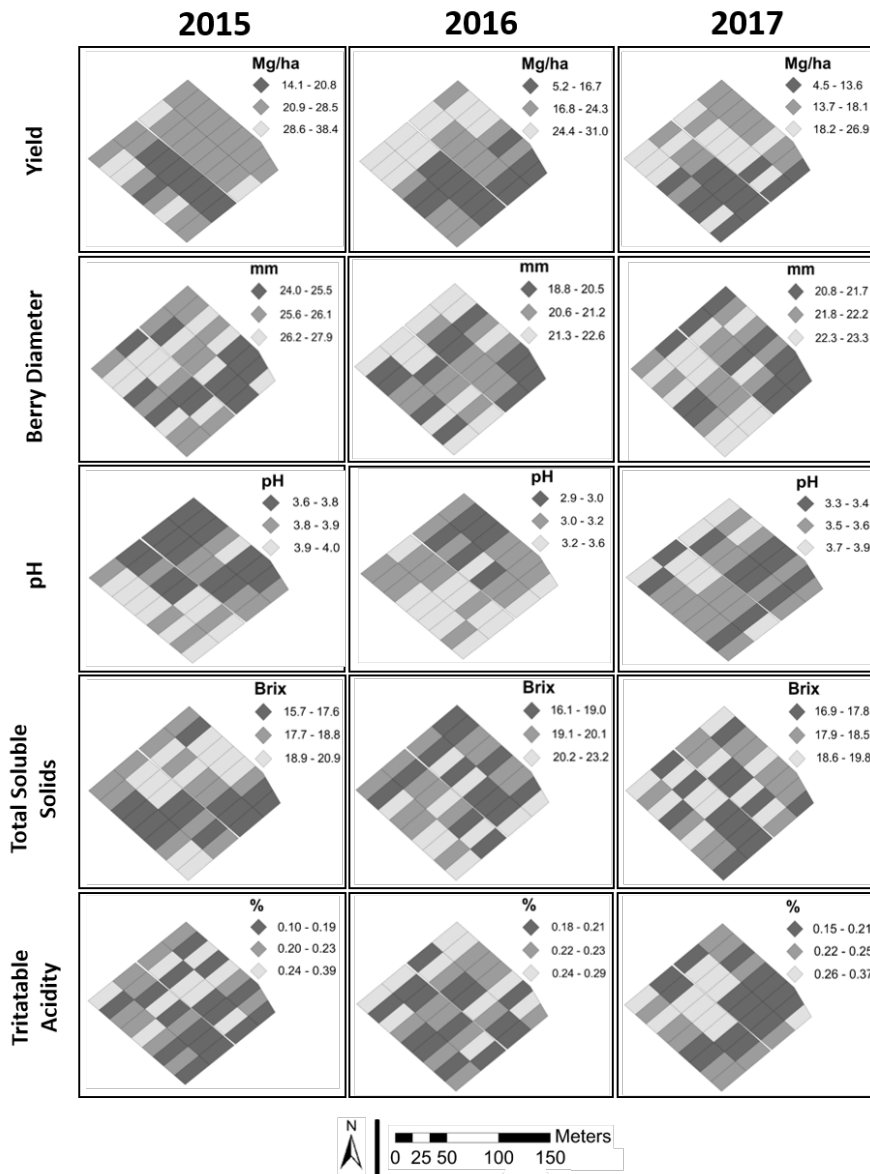


Figure 12.3: Thematic maps of Yield (top row), Berry Diameter (second row), pH (third row), Total Soluble Solids (fourth row) and Titratable Acidity (bottom row) for 2015 (first column), 2016 (second column) and 2017 (third column) to illustrate similarities and differences in variable response between years and between variables within years

indicating that in this part of the field different management practices can be applied. In addition, the spatial pattern for other quality attributes such as TSS and pH was not stable. This variation can be explained by the different weather conditions that occurred among the different years of the study.

Table 12.2 Pearson's correlation matrix between cumulative VIs and table grape yield and quality attributes.

VI	pH	TSS (°Brix)	TA (%)	Berry diameter (mm)	Yield (kg ha ⁻¹)
<i>Whole-season</i>					
cNDVI	-0.29	0.16	-0.23	0.01	0.37
cGNDVI1	0.06	0.06	-0.25	0.13	0.08
cGNDVI2	0.30	0.06	-0.23	0.63	0.52
cNDRE1	-0.28	0.11	-0.19	0.07	0.34
cNDRE2	-0.18	0.31	-0.18	0.11	0.33
<i>Pre-Veraison</i>					
cNDVI	-0.55	0.19	-0.12	-0.25	0.26
cGNDVI1	0.31	-0.20	-0.27	0.43	0.27
cGNDVI2	0.41	-0.08	-0.23	0.74	0.59
cNDRE1	-0.18	0.02	-0.15	0.17	0.37
cNDRE2	-0.26	0.21	-0.21	0.11	0.44
<i>Post-Veraison</i>					
cNDVI	0.34	-0.01	-0.21	0.39	0.24
cGNDVI1	-0.32	0.36	-0.02	-0.38	-0.24
cGNDVI2	-0.23	0.42	-0.08	-0.12	-0.03
cNDRE1	-0.34	0.27	-0.16	-0.27	-0.03
cNDRE2	0.04	0.27	-0.03	0.04	-0.03

Bold values indicate significance at $p=0.05$ level. Italics indicate VIs used subsequently (Table 12.3)

For pH the strongest correlation was with pre-veraison cNDVI ($r = -0.55$), for TSS with post-veraison cGNDVI2 ($r = 0.42$), TA with whole-season cGNDVI1 ($r = -0.25$), berry diameter with whole-season cGNDVI2 PrV ($r = 0.736$) and yield with pre-veraison cGNDVI2 PrV ($r = 0.58$). The strongest correlations were with cGNDVI and not cNDVI or cNDRE. These findings accord with other studies that indicate that the performance of other VIs might be better when compared with classical spectral VIs, such as NDVI (Hall and Wilson 2013; Anastasiou et al.

2018). Moreover, the strongest correlations with yield characteristics were for different cumulative VIs (Table 12.2). The latter agrees with the result of Anastasiou et al. (2018) who found that different crop stages have different accuracy for estimating yield characteristics of table grapes.

The linear regression models of table grape yield and quality attributes with proximally sensed cVIs showed that the model fit explained between 20 and 60% of the variance in grape quality and quantity attributes (Table 12.3). The berry diameter regression model had the best fit (adjusted $R^2 = 0.60$) and TSS the poorest (adjusted $R^2 = 0.20$). The yield estimation model explained 45% of the variance (Table 12.3). These results contradict those of Anastasiou et al. (2018) who found larger coefficients of determination when modelling table grape quality attributes, such as BD and TSS, with VIs from only one crop growth stage. This can be explained by the fact that specific crop stages, and the vigour conditions at these stages, will have different effects on final production (Sipiora and Granda, 1998; Intrigliolo and Castel, 2010). Quality in particular may be more aligned with conditions at specific stages, rather than an integration over the entire season. In contrast, absolute yield might be better explained through a cumulative approach.

Table 12.3. Linear regression models of table grape yield and berry quality with cVIs. The cVIs were selected based on correlation analysis.

Regression Model	adjusted R^2	RMSE
Yield = $-5764.59 + 11679.57 \times \text{cGNDVI2 PrV}$	0.45	3.64 Mg ha ⁻¹
BD = $\sqrt{(253.84 + 51.86 \times \text{cGNDVI2 PrV}^2)}$	0.60	1.2 mm
TSS = $11.39 + 3.65 \times \text{cGNDVI2 PoV}$	0.20	0.7 °Brix
TA = $0.56 - 0.09 \times \text{cGNDVI1}$	0.20	0.02 %
pH = $1/(0.951 - 0.551 \times \ln \text{cNDVI PrV})$	0.42	0.01

PrV=pre-veraison, ; PoV = post-veraison

The various cumulative VIs used in this study resulted in different performances with the cumulative VIs based on GNDVI having the strongest correlations with the most variables (yield, BD, TSS and TA). This accords with Anastasiou et al. (2018) who found that both proximally- and satellite-derived single crop stage GNDVI produced better results than NDVI. According to their study, this can be explained by the saturation of NDVI values, which resulted in smaller estimates of crop yield characteristics. Furthermore, the cumulative VIs had poorer accuracies than single stage VIs from the same study (Anastasiou et al. 2018). This is because the various agricultural operations (e.g. irrigation, canopy trimming) that take place during the crop growth periods decrease the within-field spatial variation and smooth the values of the cumulative VIs. Finally, this study accords with that of Sun et al. (2017)

and Mirasi et al. (2019) who found that cumulative VIs can assess crop properties better, such as yield, when compared to single crop stage measurements.

Conclusions

In this study, an assessment of proximal sensed cumulative VIs for the estimation of crop yield and quality characteristics was conducted during three crop growing seasons (2015, 2016 and 2017) on a commercial table grape vineyard in Greece cultivated with Thompson Seedless variety grapes.

The cumulative VIs based on GNDVI presented higher correlations with yield, BD, TSS and TA when compared with other cumulative VIs. Moreover, the results indicated that cumulative VIs have the potential to become a tool for assessing table grape characteristics and thus being used on management zone delineation for selective harvesting. However, cumulative VIs must be carefully used as they might not be suitable for estimating specific attributes under intensive management conditions when frequent agricultural operations occur in the field. In this situation, single stage VIs may exhibit stronger relations and be more useful for management.

Case Study 12.2. Airborne multispectral images as a tool to characterize the spatial variation of vine water status: application to a non-irrigated Mediterranean vineyard

Introduction

The evolution of vine water status (VWS) throughout the vineyard growth cycle has a direct effect on grape composition and harvest quality through its influence on fruit growth, yield, and fruit metabolism (Dry and Loveys 1998; Ojeda et al. 2002). Therefore, it is important to monitor VWS, to predict either expected harvest quality or as a source of critical information for vineyard management, under both irrigated and non-irrigated conditions (Naor et al. 1997; Choné et al. 2001).

Several reference methods have been proposed to measure VWS; Leaf Water Potential (LWP), Stem Water Potential (SWP) and Predawn Leaf Water Potential (PLWP) (Sibille et al. 2007). These methods are widely used, but they are laborious manual techniques, requiring specific instrumentation and a certain level of skill when making measurements (Ojeda et al. 2002; Sibille et al. 2007). These constraints make systematic Spatio-Temporal (S-T) VWS measurements with these methods time-consuming and difficult to perform. For this reason, these reference measurements have been used mainly to monitor the temporal change in VWS at only a few locations within vineyards. The VWS observations therefore tend to be

reported at a low spatial resolution and often under an assumption that VWS is homogeneous over the measurement area (i.e. the block or set of blocks are assumed to behave similarly).

However, VWS can be highly variable within blocks, within vineyard estates (Taylor et al. 2010) and across viticulture regions (Baralon et al. 2012). So, characterizing the spatial variation of VWS is key to improving the positioning of reference measurements to enable managerial decisions based on the observed spatial patterns (Acevedo-Opazo et al. 2008a). Availability of soil water, because of differences in soil depth and soil physical properties is a key influence on VWS. Under non-irrigated Mediterranean conditions, water restriction decreases the vegetative growth of the vine (Celette and Gary, 2013), so vine vigour should constitute an indicator of the spatial variation in VWS.

This case study illustrates the use of a vegetation index, obtained from multi-spectral aerial images, to assess the spatial variation of VWS under non-irrigated Mediterranean conditions. The aim was to verify that remotely sensed vegetative indices are a useful auxiliary data layer for understanding and managing viticulture practices according to the spatial variation of VWS.

Materials and methods

Description of the vineyard

The study vineyard is at Pech Rouge (Gruissan, Aude, France; 43°08'30"N, 3°07'30"E). It has 28 blocks with a total area of ~32 ha. The vineyard is representative of vineyard diversity in southern France in terms of training systems (vertical shoot positioning and gobelet), the age of vines (from 2 to > 50 years old) and varieties (*Vitis vinifera* cv Syrah, Grenache, Chardonnay, Petit Verdot, Muscat, Mourvedre and Carignan).

Management practices (pruning, fertilization, trimming, mechanical weeding, etc.) were very similar for all blocks. The vineyard is non-irrigated and has a Mediterranean climate with a hot dry summer. Precipitation occurs mainly in autumn and spring. A large evaporative demand usually leads to considerable vine water restrictions in summer. Examples of average water constraint over the vineyard, estimated by PLWP, were -0.75 MPa in August 2003 (a very dry year) and -0.60 MPa in August 2006 (a wet year) (Taylor et al. 2010).

Multispectral Image

Aerial images (1 m² pixels) were collected by l'Avion Jaune (Montpellier, Hérault, France) at veraison (August, 2006). The spectra included were: (i) blue (445–520 nm), (ii) green (510–600 nm), (iii) red (632–695 nm) and (iv) near-infrared

(757–853 nm). The NDVI was derived for each image after the 1 m² pixels were aggregated into 3 m² pixels using the methodology outlined in Acevedo-Opazo et al. (2008b). This approximates the ‘mixed pixel’ row spacing approach of Lamb et al. (2004). Data mapping was performed using QGIS 2.18. Three classes of NDVI were created; high, medium and low relative to the tertiles in each individual block.

Spatial variation and vineyard block selection

Not all blocks had the same magnitude of spatial variation of NDVI. Vineyard managers will focus on blocks that show considerable variation and with spatial patterns large enough to justify the use of site or zone-specific practices. To determine blocks that would be most appropriate for site-specific management, the Technical Opportunity Index (TOi) (Tisseyre and McBratney, 2008) was used to rank them. It was computed for each block with the GeoFIS freeware (Leroux et al. 2018). The TOi ranks were used to meet two objectives: 1) to identify blocks that could justify zone-specific management and 2) to target blocks to collect additional data from.

Sampling scheme

Sampling sites were selected based on the NDVI information. Only blocks with a large potential for zone-specific management (large TOi values) were considered. For the selected blocks, two zones were selected corresponding to a relatively high and a relatively low NDVI response, with a constraint that the selected zones presented a significant area in the block (> 100 m²). This last criterion was considered mainly for practical reasons, to ensure that the number of vines in each zone was relevant for further analysis. A measurement site of 40 m² was randomly located within the selected high and low NDVI zones (2 sites per block). Zones of medium NDVI values were considered transition zones and not sampled.

Vine measurements

Two types of measurement were performed to verify the origin of the difference in NDVI values: vine vegetative expression, using the external canopy area (ECA) per vine (m² pl⁻¹), and PLWP (MPa) measured at veraison, when the water stress was assumed to be at its strongest for the season. The ECA was estimated manually over five vines along the row using measurements of canopy height (m) and width (m). The PLWP was measured over the same five vines between 3:00 and 5:00 a.m. using a pressure chamber (Scholander et al. 1965).

To identify the possible uses of the NDVI in relation to VWS, a more intensive temporal survey of PLWP coupled with harvest measurements was performed on

the two NDVI zones in Block 5. This block was chosen as it had a large TOi value and was considered a block with potentially high fruit quality by the manager. Zone-specific management may therefore be important to improve yield and quality. The PLWP was measured on seven dates during the season. At harvest, variables were measured to characterize production (yield vine⁻¹) and berry quality. Quality measurement from both the high and low NDVI zones were based on 10-bunch samples (from different vines). Soluble solid concentrations (using a thermo-compensated refractometer) (°Brix), total acidity (g L⁻¹ of sulphuric acid) and pH were measured at berry maturity. Total extractable anthocyanins and total polyphenols index were assessed at harvest using the methodology proposed by Iland et al. (2000).

Results

The 3-class NDVI map shows that all blocks have spatial patterns corresponding to low, medium or high NDVI values (Fig. 12.4). However, some blocks have larger, more contiguous NDVI zones. It is possible to identify geometric patterns (rectangles, squares) that correspond to experiments within blocks related to different rootstocks and or different training systems. Other blocks (with no experiments) had zones with more complex, irregular shapes. These zones are likely to be related to environmental characteristics (soil, topography, and so on). The vineyard manager wanted to focus on these blocks to consider different practices for better control of yield and berry quality at harvest. Recall that in this non-irrigated vineyard, the assumption is that the variation in the NDVI values makes it possible to estimate the variation of vegetative expression induced by differences in VWS.

The TOi opportunity index was calculated to rank the blocks according to the within-block variation in NDVI and to identify three classes of blocks (Fig. 12.5). There were 13 blocks that had strong and structured spatial variation in NDVI (in white on Fig. 12.5). The vineyard manager's expertise reduced this to 11 blocks as two blocks (Blocks 12 and 13; Fig 12.5) showed significant variation caused by experiments related to the training system or the rootstock. The rest of this case study focused on these 11 blocks, whose variation was assumed to originate from environmental factors.

With aerial NDVI collected over 3 years, the 11 blocks showed a relationship between the EC_a ground measurements and the NDVI up-scaled to 3 m² pixel ($R^2 = 0.64$, $n = 33$, data not shown). Similar findings have been found in California, USA (Johnson et al, 2003). It confirmed that NDVI was a reliable indicator of the variation in vegetative expression within blocks in these specific production conditions.



Figure 12.4: Vineyard blocks at Pech Rouge with the NDVI layer classified into three equal classes (tertiles) within-blocks.

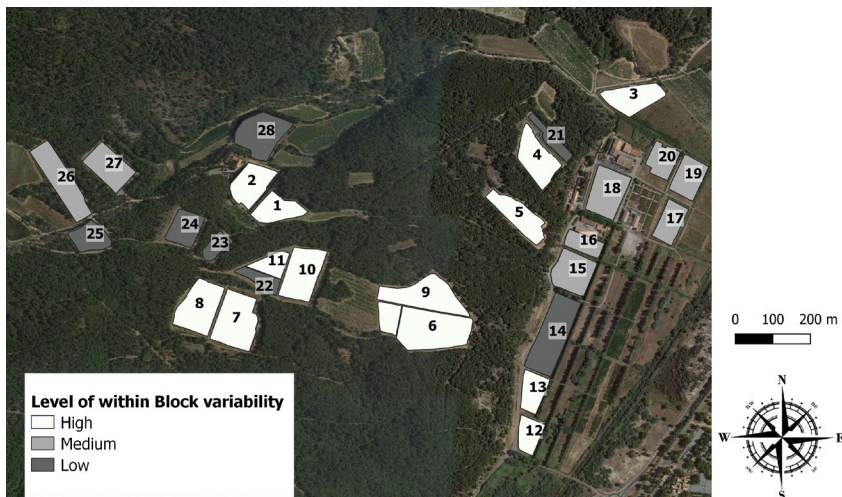


Figure 12.5: Classification of the blocks according to their variability in NDVI response as assessed using the TOi metric. Block IDs are shown that relate to Block IDs referred to in the text and in Fig. 12.6

The variation highlighted by the NDVI was mainly explained by water access and the resulting PLWP (Fig.12.6). Of the 11 selected blocks, the observed PLWP at veraison was systematically smaller in the zones of low NDVI. The differences were particularly significant ($p < 0.05$) for Blocks 3, 4, 5, 6, 7, 8 and 9 on calcareous soils. The differences are less, but still significant ($p < 0.05$), for Blocks 10 and 11 on colluvial soils. For Blocks 1 and 2 on sandier soils, the differences in PLWP

were small ($p > 0.05$) between NDVI zones. However, for these last two blocks, the general trend was followed, with smaller PLWP (more water stress) associated with smaller NDVI values.

Although NDVI proved to be interesting auxiliary information for mapping the spatial variation of VWS, Fig. 12.6 emphasises that any analysis must be supported by expert knowledge of the soil type and block conditions. For example, it would have been irrelevant to propose a linear model of water stress as a function of the NDVI at the whole vineyard level given the different responses observed on different soil types.

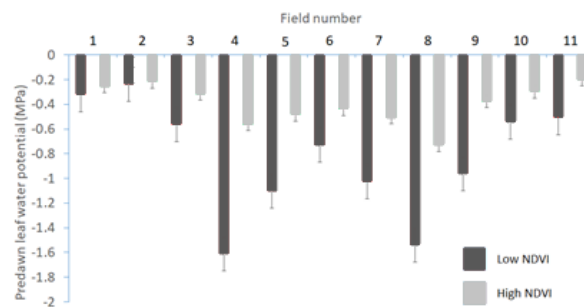


Figure 12.6: Predawn Leaf water potential observed at within block sites corresponding to high and low NDVI values over 11 blocks (veraison). Field numbers refer to blocks indicated in Fig 12.5.

Figure 12.7 shows the VWS results from Block 5 where the PLWP was monitored simultaneously in both NDVI zones (low and high) on 7 dates throughout the season. During the summer, evaporation demand was large, but water consumption by the vines was not compensated for by either irrigation or rainfall. However, water restriction remained moderate in the high NDVI zone where the soil water capacity must be greater. In contrast, in the low NDVI zone, considerable water restriction was observed from early in the season, which can be explained by a relatively smaller soil water capacity. The NDVI zones therefore made it possible to highlight likely differences in soil water capacity. However, the depth of vine roots in these non-irrigated plots (> 5 m) and the difficult soil conditions in which to dig makes it difficult to support this hypothesis with more objective observations. These technical difficulties argue in favour of the use of a simple observation, like NDVI, to integrate and explain varying vine growth conditions.

In Figure 12.7 the differences in VWS between the high and low NDVI zones were apparent from the beginning of the season and increased as the season progressed. Since it has an impact throughout the season, from flowering to grape maturation, this difference affected the growth of the vines (which explains differences in NDVI values) at the beginning of the season and the quality of the harvest during ripening (Table 12.4). The low NDVI zone had less sugar, less phenolics and more

acid at harvest than the high NDVI zone. All three conditions are known to reduce the potential quality of any wine produced from the grapes. These values indicated that the low NDVI zone had a problem achieving crop maturity, resulting in poorer berry quality.

The knowledge of within-block variation explained by water stress and highlighted by NDVI zoning justified the implementation of several applications in the vineyard: i) targeted sampling to estimate yield, maturity and harvest date better, ii) some experiments to assess site-specific mechanical weeding in the inter-row to decrease competition for water and iii) irrigation combined with appropriate nitrogen fertilization on blocks with very variable NDVI. Differential harvest has not been implemented because of logistical constraints.

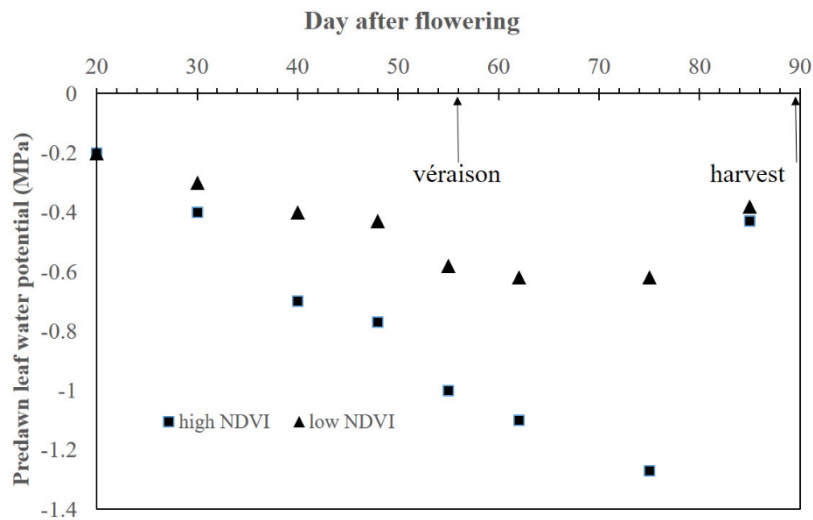


Figure 12.7: Evolution of vine water stress (measured as predawn leaf water potential (MPa)) over a season for two sites stratified between a low (▲) and a high (■) NDVI zone in Block 5. Arrows and labels indicate key crop stages.

Table 12.4: Mean berry quality attributes at harvest for two NDVI zones (High and Low) in Block 5.

Zone	Sample size (n)	Sugar (g l ⁻¹)	pH	Acidity (g l ⁻¹)	Total polyphenol index (TPI)
High NDVI	29	22.55	3.81	3.54	36.9
Low NDVI	20	20.89	3.78	3.99	33.66

Conclusion

In a non-irrigated Mediterranean context, this case study showed the value of NDVI in mapping vegetative expression and explaining the variation in VWS because access to water is the main factor affecting vine growth. The aerial NDVI was an ‘easy-to-acquire’ data set that made it possible to highlight zones of different water stress easily and with high spatial resolution. The case study also highlighted the limits of the approach. The NDVI/water stress relation shown here is only relevant in this pedo-climatic system and the results cannot be extrapolated directly to all vineyards. This case study is a reminder that NDVI remains an integrative data source for summarizing how environmental factors and operations affect the canopy. Its interpretation for decisions must be systematically based on knowledge of the ecophysiology of the vine and with local soil expertise. For significant water constraints, the study shows that the variety effect is negligible compared to the effect of environmental factors. However, the interpretation of NDVI values to quantify differences in water stress remains difficult without prior expertise on soil conditions and especially without taking into account the characteristics of the field (training system, planting density, grass cover, etc.) likely to affect NDVI values.

This research has contributed to the launch of commercial services specifically dedicated to remote sensing in viticulture: in particular the Oenoview service (Teranis, ICV, France). Although constantly increasing, the use of remote sensing in viticulture remains marginal in France, it represents about 1% of the area planted with vines (Lachia et al. 2019). The most important use (in terms of area) concerns cooperatives faced with a great diversity in vineyard blocks spread over a large area. For these structures, the benefit from maps of vegetative expression at veraison is an interesting source of information for the qualitative selection of blocks for improving yield and quality estimates before harvest. In this respect, in the vineyards of southern France, knowledge of the within-field spatial variation controlled by water restriction is relevant to rationalize and optimize the positioning of observations in the blocks before harvest.

Case Study 12.3. Proximal Sensing for Cotton Management

Introduction

Cotton (*Gossypium* sp.) is one of the most important fibre crops, with approximately 35 million ha grown worldwide, making it one of the 20 most important global commodities in terms of its value in 2016 (<http://www.fao.org/faostat>). Among the top producers, production in China, India and Pakistan is mainly by small farmers in labour intensive crop systems, whereas production is highly mechanized in the USA, Brazil and Australia. In these latter countries, the cropping systems are capital intensive and require many interventions throughout the season.

Cotton is a perennial plant that is cultivated as an annual crop. It has a growing season of approximately 180 days. If the crop goes through severe biotic or abiotic

stresses in this period, the plant will drop most of its reproductive structures as a self-preservation mechanism (Stewart, 2009). If, however, conditions are very favourable, the (perennial) plant will prioritize vegetative over reproductive development, a scenario known as rank growth. Although domestication, selection and breeding have produced cultivars with characteristics more aligned with growers' needs, crop management still plays an important role in fibre quality and yield. The main factors controllable by growers that affect productivity are irrigation, fertilizer (mainly nitrogen) and plant growth regulators (PGR). The PGRs are used to control growth, promote higher yields, better fibre quality and permit mechanical harvest.

The optimal rate of PGR application depends on crop height, biomass, and growth rate and these are influenced by variable environmental conditions. Given known variability, there is a great interest in using remote and proximal sensors to monitor crop development and to guide variable-rate application of inputs. Active and passive optical reflectance sensors mounted on various platforms can detect infield crop variation (Sui et al, 2012; Trevisan et al, 2018). Sensors have been used to predict biomass, plant height, height-to-node ratio, nitrogen nutrition status, crop maturity and lint yield (Portz et al, 2014; Arnall et al, 2016). The performance of sensors can vary throughout the crop season because of crop canopy changes and management practices. Some limitations of optical sensors have been observed when used later in the season, related to the known effect of signal saturation with dense canopies and changes in the spectral signature of the plants (Mutanga & Skidmore, 2004). Unlike optical readings, crop height and volume observations have shown good relations with crop biomass through the entire season, without saturation effects. The aim of this case study is to evaluate the potential uses of several proximal sensors as tools to monitor cotton development and yield.

Material and Methods

Observations were taken from 10 fields over 4 years in two states in Brazil (Goiás in 2013 and 2014 and Mato Grosso in 2015 and 2016). The soil in the fields ranges from clay Oxisols to sandy loam Quartzipsamments (Leão, 2016), with different levels of spatial variation in clay content.

Information on soil spatial variation was provided by an apparent soil electrical conductivity (EC_a) survey of the 0–0.3-m layer using a Veris 3100 system (Veris Technologies, Salina, Ka, USA) on 12-m swaths and georeferenced using real-time kinematic (RTK) Global Navigation Satellite System (GNSS) receivers. The EC_a data were acquired in January (in the rainy season), between the soya bean harvest and cotton planting. Data processing consisted of interpolating the EC_a and elevation data by ordinary kriging. A digital elevation map was used to extract the topographic derivatives slope, aspect, curvature and topographical wetness index. Ten points representing the full range of EC_a variation in each field were chosen for soil

sampling. The EC_a values at these points were compared with laboratory soil particle size analysis to generate clay and sand maps for each field.

In-season monitoring of crop vigour was done by two types of proximal optical sensor systems. The first optical sensor system, OPS1 (N-Sensor™ ALS, Yara International ASA, Dülmen, Germany), was installed above the vehicle cabin and readings were taken from an oblique position. The N-sensor measures canopy reflectance in the red edge (730 nm) and near-infrared (NIR) (760 nm), and a scaled logarithmic difference of reflectance at the two wavelengths was used as the vegetation index in all comparisons (Jasper et al, 2009). The second optical sensor system, OPS2 (Crop Circle ACS-430, Holland Scientific, Lincoln, NE, USA), was mounted to take readings directly above the crop canopy. The OPS2 was integrated with the GEOSCOUT GLS-420 (Holland Scientific, Lincoln, NE, USA) for data acquisition. The CropCircle sensor measures canopy reflectance at three wavelengths, but only the red edge (730 nm) and NIR (780 nm) were used to calculate the Normalized Difference Red Edge Index (NDRE) (Horler et al. 1983), which was used in all comparisons.

In-season proximal monitoring of plant height was done using a georeferenced ultrasonic system, US1 (HC-SR04, generic sensor), mounted in the same position as OPS1. The system was developed for this research, using low-cost hardware commonly used in automation projects and data acquisition based on an Arduino® Mega 2560 (Arduino, Ivrea, Italy). The time of flight principle was used to measure the distance between the top of the canopy and the sensor (at a fixed height above the ground). Finally, a terrestrial 2-D light detection and ranging scanner system (LiDAR–LMS200, Sick, Waldkirch, Germany) was mounted at the front of the vehicle 3.0 m above ground level. Customized data acquisition software was developed to collect georeferenced LiDAR data. The LiDAR sensor was programmed to collect data with an angular resolution of 1° , an angular range of 180° and a distance range of 80 m. The distance resolution was set to 0.01 m. The acquisition rate was 75 Hz, achieved by configuring a 500 kbps baud rate communication through a RS422 serial interface. Returns further than 24 m were excluded, and distances and angles were used to calculate the UTM coordinates of each return point. The data were subsampled to obtain a constant spatial density because the raw data were denser closer to the machine path. The point cloud was used to extract the ground and canopy levels, defined as the 5th and 95th percentile of the values within 1 m. Plant height was then obtained by subtraction.

All sensors were installed on a high-clearance vehicle operating with a swath width of 24 m, at a maximum travel speed of 6.4 m s^{-1} (23 km h^{-1}). All sensor data acquisition was made simultaneously in a single machine pass in each field. Cotton was harvested using a JD 7760 cotton picker (John Deere, Moline, IL, USA), with the Harvest Doc™ yield monitoring system. All data were georeferenced using RTK GNSS. All sensor datasets were filtered to remove local extreme values (Spekken et al. 2013). The point data were interpolated to a common grid with 1-m spatial resolution using inverse distance weighted. This method was preferred as the data were already dense and it required less computational effort. All maps were

prepared using QGIS software (QGIS Development Team 2018). All statistical procedures were performed using the R programming language (R Core Team 2018).

Results and Discussion

General observations

Data acquisition was successful, and there were no major problems with the sensors. A few problems were reported with the custom-built systems, mainly wiring and some software problems. The commercially available optical systems operated consistently over the four years of data acquisition. The robustness of the sensors is one of the main concerns of growers when considering the adoption of new technologies, therefore this was a very positive result.

The performance of the sensors was better when the variability in crop development had longer spatial ranges and less short-scale variation. Usually the large regions with larger or smaller values have similar patterns, but the pass to pass differences in one map did not match the same short-scale variation in the others (Fig. 12.7). The practical implications of this result is that choice of the best sensor and prescription protocol will depend on the resolution at which any variable-rate prescription can be applied for each particular input. There was also a temporal trend in the proportion of short-scale variation, which was greater in the early stages of the crop because of uneven crop emergence. This made the footprint of the sensor and the ability to average short-scale variation more important at this stage. The OPS1 had an advantage in these early stages (Trevisan et al. 2018) due to its oblique angle of operation enhancing crop reflectance and minimizing soil reflectance compared to sensing the crop from a top-view angle (OPS2). The temporal stability of the spatial variability is also related with its scale. In general, the long-range variability was more stable over long periods of time and different crops in the same field, while short-scale variation was largely affected by operational quality and the interaction with pests and diseases.

Example field

We chose one field from the 2015 crop season to describe the sensor results. The field was 70 ha with a sandy loam soil and clay content ranging from 50 to 150 g kg⁻¹. This was not the most representative field for cotton production in the region, as usually soils with higher clay contents (> 350 g kg⁻¹) are preferred. Nevertheless, considerable crop variability at both short and long ranges made it a good choice to compare sensor performances. The sandy soils are more fragile and small differences in organic matter and nutrient availability can have a large influence on crop development. The EC_a map gives an idea of soil variability over the field (Fig.

12.7a). The density of points collected was approximately 200 points ha⁻¹. The EC_a was very small, reflecting the low cation exchange capacity of this soil. The eastern half of the field had predominantly smaller EC_a and sandier soils, while the western half had larger EC_a and clay content.

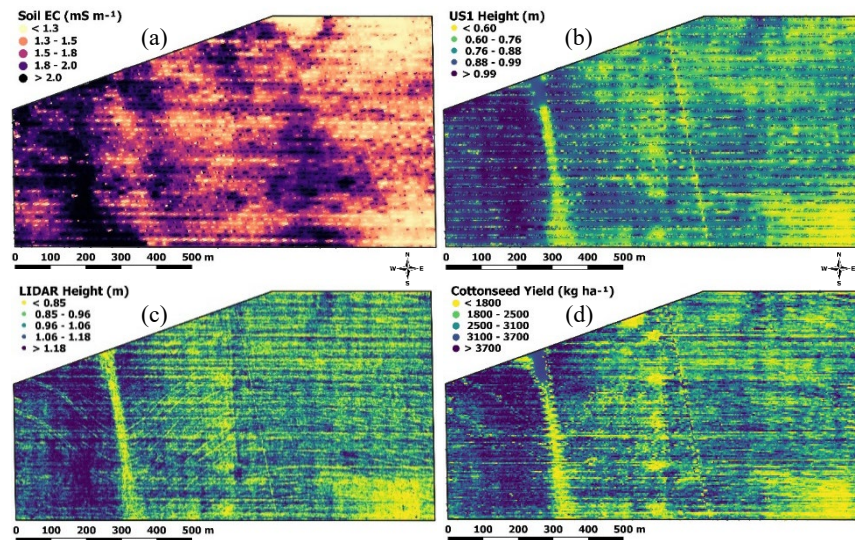


Figure 12.8. Spatial distribution of the soil electrical conductivity from the Veris 3100 sensor (a), final crop height measured by an ultrasonic sensor system (US1) (b), final crop height measured by a LiDAR sensor system (c) and cottonseed yield (d).

The final crop height measured by US1 (Fig. 12.8b) showed an overall similarity with the EC_a map. The density of points was approximately 1800 points ha⁻¹. However, they were all concentrated around the machine path, representing an effective sample of only four crop rows in every 30 rows. The correlation between crop height measured by sensors and by traditional hand-based methods was strong when evaluating small plots (Sui et al. 2012; Trevisan et al. 2018). There was a clear trend of taller plants in the western half of the field and smaller plants in the centre and eastern parts. The stripe with small plants on the western side was associated with the topography of the field. This region has a depression and was the preferred path for run-off water. Heavy rain events (> 100 mm hour⁻¹) caused soil erosion and crop lodging in this area. The narrow strip of small plants in the centre was created artificially one month before harvest because of the need to install a pipeline across the field, which required plants to be removed.

The errors observed in the US1 were higher at the early crop stages because of the machine path error, making positioning of the sensors directly over the canopy more difficult (Trevisan et al. 2018). There were also systematic errors observed

related to changes in the machine dynamics. The air suspension and tyre compression in the soil gradually changed as the input tank was emptied, altering the relative height of the fixed mounted sensor to the canopy. Irregularities in the terrain topography and machine inclination could also contribute to the error. These challenges would be greater if the sensors were installed on a boom with additional difficulties in calculating the distance to the ground from a moving (swaying) boom.

The same general patterns of crop height observed for the US1 sensors can be seen in the LiDAR map (Fig. 12.7c). The density of points is larger, approximately 600,000 points ha^{-1} in the raw data and 5,000 points ha^{-1} in the final height map. The greater resolution allows better identification of short-scale variation and visualization of some patterns that were not clear in the US1 map. The presence of shorter plants following the contour levels of the terrain were probably related to earthworks used to control soil erosion. The stripes along the direction of seeding are related to unequal emergence associated with planter effects at sowing.

The LiDAR system outperformed the ultrasonic system in mapping crop height. There were always sufficient points at survey times to determine the ground level, therefore the absolute position of the sensor was not needed to calculate crop height. It may become a limitation if the canopy achieves full cover and the laser is unable to determine the ground level. The cost of the LiDAR system (hardware and processing requirements) is an order of magnitude higher than the US1, therefore the economic advantage of this system will depend on the use of the data. Currently, the management of spatial variation is usually limited by the resolution of the variable-rate applicators rather than the sensing capabilities, which makes it more difficult to take advantage of the higher resolution data generated by the LiDAR.

Similar results and resolution could be obtained with a UAV and photogrammetric tools. The main challenges at the moment for the use of UAV imagery are in the general logistics of collecting UAV data, the time needed to process images and to make the data available for prescription applications, the accuracy of the GNSS used and the need for ground control points (Feng et al. 2020)

The yields were generally small (Fig. 12.8d), compared to the national average of 3,800 kg ha^{-1} (CONAB 2015), mainly because of the sandier soils and poor crop establishment. There was a reasonable positive correlation (> 0.5) between yield and crop height measured by both sensors (Table 12.5). This correlation will not always hold true and will depend on local growth characteristics.

The correlation of EC_a with yield is a good indicator of the proportion of variability that is likely to be stable over the years, since EC_a patterns tend to be stable (Guo 2018). The EC_a map could be used to adjust seeding rates according to variable soil conditions. The general recommendation is to apply larger seed rates in sandier soils and reduced rates in heavier (clay) soils. This promotes some compensation as the plants in sandier soils tend to have a reduced development, and therefore a smaller number of reproductive structures per plant.

The stronger correlation of yield with the LiDAR height compared with the US1 height is mostly explained by the sources of errors previously discussed in the US1 data collection. Although the sensor resolution may be important to obtain better

estimates of infield variability, the best economic results will be observed when the sensing resolution and the application resolution are matched (Amaral et al. 2018). The LiDAR data showed significant short-scale and row-to-row variation. Variable-rate application at this resolution is still not practical because of the lack of resolution in the appropriate equipment, being either too expensive or too complicated to be adopted by farmers.

Table 12.5: Correlation matrix for soil and crop attributes in a cotton field.

	Yield	EC _a *	US1 Height
EC _a	0.38		
US1 Height	0.51	0.52	
LiDAR Height	0.61	0.46	0.57

EC_a: Apparent soil electrical conductivity; US1: Ultrasonic sensor system.

Other research has demonstrated that when fields can be divided into management zones and long-range variation dominates, low-cost systems of variable-rate application have produced good results. In this scenario, PGRs can be applied effectively, resulting in more uniform cotton plant height and yields within fields (Baio et al. 2018). To show the economic viability of investing in a more expensive system is difficult. The economic return of investment of each technology will depend on the degree of variation in each field and the ability to take advantage of it with site-specific applications. It is usually easier to show the benefits with product savings than with significant differences in crop yields. It is even more challenging to show consistent differences in fibre quality (Trevisan et al. 2018).

The main challenge that remains for the use of proximal sensors in cotton management is related to the lack of agronomic knowledge and algorithms to convert sensor readings into decisions and prescriptions. The sensors provide information that is well correlated to the spatial variation of crop development or nutritional status. But to make the right decisions information on the crop response to the input that will be applied is required. For example, cotton biomass in the early stages may be more affected by population counts than by nitrogen deficiency. These confounding factors make it difficult to make the right decision based on a single evaluation from a crop canopy sensor. Combining multiple sensors and readings from different crop stages can certainly improve the prescriptions (Sharma et al. 2016). The use of calibration strips and on-farm precision experiments can further improve the results, accounting for the temporal and regional variability of crop response to any input (Arnall et al. 2016; Kindred et al. 2017).

Further evidence of this challenge is the wider adoption of solutions as services instead of products (sensors). Even though having the sensors installed on the agriculture machinery has a lower operational cost than using a dedicated platform to collect the data, the services approach has been more successful because it allows more flexibility and less disruption of the field operation. It is also easier to combine

more sources of information and agronomic knowledge when the prescription is done as a separate step rather than in real-time (Trevisan et al. 2018).

Furthermore, the variable-rate application of PGR alone is not enough to manage spatial variation when there are large soil differences (Trevisan et al. 2018). The use of variable-rate seeding, nitrogen and PGR applications needs to be planned in an integrated manner to maximize the economic result in every part of the field. However, combining multiple sources of information to guide decisions about multiple inputs under many uncertainties is not a trivial task. This requires better software and more complex models. Sensor fusion and autonomous decision-making techniques are likely to benefit from machine learning methods that have been applied to many domains (Chlingaryan et al. 2018).

Conclusions

Crop sensors showed good performance for monitoring within-field variability in cotton height and vigour (biomass) in fields. There are sensors available with different resolutions and working principles, which might perform better in different cases. Integrating temporal information and multiple sensors is important for improving results. Local farmers have access to sensors available in the market and some already use them for nitrogen management. Challenges remain with agronomic knowledge and algorithms to convert the sensor readings into decisions and prescriptions. The high value and large-scale production of cotton associated with innovation-oriented producers in Brazil make this crop ideal for developing and experimenting with new technologies.

The availability of variable-rate applicators that match the scale of variation is also important. Managing all the inputs in an integrated framework allows for better crop management. Spraying solutions remain a challenge, not because of a lack of technology, but because of the cost associated with this technology for the variable-rate application of multiple products required in certain situations. Further research is needed to evaluate the return on investment of different technologies.

Case Study 12.4. Integration of UAV imagery into potato crop modelling services

Introduction

The increased availability of unmanned aerial vehicles (UAVs) has significantly increased the ability of growers to acquire imagery of their crops. Previously, growers had to rely on satellite imagery (with resolution, over-pass time and cloud cover

issues) or aerial surveys, which are often expensive, to obtain imagery. The availability of UAVs has allowed growers greater flexibility with high-resolution image acquisition. They can be operated by growers to collect information when needed. A UAV system still has limitations. However, there are some limitations that initially revolved around converting multiple images of a field automatically into a 'mosaiced' image of the field. Algorithms have advanced recently and growers can now acquire timely, mosaiced, geo-rectified images of whole fields without needing any specific image processing skills. This means that UAV imagery is now a viable information source for modern commercial agriculture (Tsouros et al. 2019, Cucho-Padin et al. 2019). The next major limitation is the cost of the system, particularly the camera. A UAV itself is just a platform, like a tractor, airplane or satellite, onto which a sensor can be mounted. The more advanced the sensing system, the more expensive it is. It is possible to mount multi-spectral (MS), hyperspectral (HS) and thermal sensors onto UAVs, however, for most growers, especially small-holder farmers, the cost of these sensors is prohibitive (Cucho-Padin et al. 2019). The 'sensor' that is accessible, is a simple colour (RGB) camera. Ideally, a MS sensor with a NIR band would be preferable for mapping vigour in a similar way to MS sensors mounted on satellites or tractors (as illustrated in previous case studies in this chapter). It is likely that such MS camera systems will become available at a competitive price point for the majority of growers; however, in the interim the use of colour imagery and of very high-resolution images is challenging for a UAV-mounted RGB camera to deliver.

Another advance in precision agriculture is the use of crop models for short-term spatial prediction (Chen et al 2017). This shifts traditional (semi-)deterministic models from long-term strategic applications (e.g. climate change predictions) to short-term tactical application for variable-rate management. This transformation requires a change of input information, and in some cases a change in parameters, within the crop model to allow newly accessible digital information, like UAV imagery, to be used. This case study illustrates how basic colour UAV imagery, has been incorporated into an existing potato model to

- a) improve functioning of the model, and
- b) allow the model to be spatialized within a field

The research and extension was performed and developed within commercial systems and led primarily by industry.

The Crop Model

The growth model in this study simulates daily crop growth of a single potato plant and its interaction with the local environment. It predicts both potential crop yield and the yield under restricted water conditions with the assumption of adequate, non-limiting nutrients and correct crop protection practices. It originates from experimental work done at the James Hutton Institute (MacKerron and Waister,

1985 and MacKerron, 1985). The model is mechanistic, modelling the sequential stages of crop sprouting, leaf expansion, dry matter accumulation and partitioning, and crop senescence of a potato plant as well as their effects on crop yield. Plant development is primarily influenced by weather factors (temperature and solar radiation interception) and soil moisture conditions (MacKerron et al 2004). Plant density information is then used to scale the plant model to a field response. The flow of the crop modelling process, and the input and intermediate parameters and variables, is shown in Fig. 12.9.

As the model is deterministic, errors at early stages of the model related to crop development will have an effect, and in some cases a large effect on final yield prediction. For example, dry matter accumulation may be up to $1 \text{ t ha}^{-1} \text{ day}^{-1}$ mid-late season. Errors in modelling the emergence date can therefore affect the predicted yield at crop burn-down by effectively shortening or lengthening the growing season within the model. For strategic, long-term uses, these errors are not critical. The model is only being used for scenario-testing and the emergence date error would be a constant. However, for short-term tactical uses, yield predictions need to be as accurate and precise as possible, and a 4–7 day difference in emergence date (model vs observed) will introduce a large error in yield prediction.

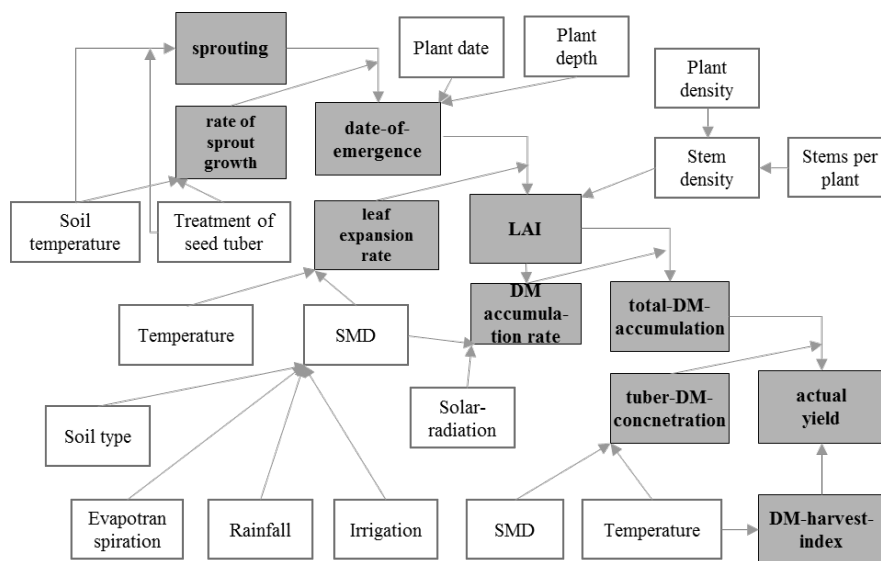


Figure 12.9 Schematic diagram of a potato crop model. The white blocks show initial conditions and other model inputs for model simulation. The grey blocks represent the progression of crop growth and development from sprouting, emergence, vegetative development to actual yield. LAI = Leaf Area Index, SMD = Soil Moisture Deficit, DM = Dry Matter.

Adapting the model using UAV imagery

The model is essentially a dry matter accumulation model, therefore, having the correct canopy size (Leaf Area Index - LAI) at any given period is critical to good model predictions. The ability to operate UAVs and process imagery at high temporal resolutions provides an opportunity to gather relevant ground cover (%) information to validate and correct the model. The model has been adjusted in three fundamental ways with observed ground cover to align the model outputs more closely with local conditions;

- 1) Early-season imagery allows identification and counting of individual plants to provide spatial plant density,
- 2) Multi-temporal early-mid season imagery can be used to either identify emergence data or to model emergence date, and
- 3) Multi-temporal early-mid-season imagery can be used to identify the date of canopy closure or the observed level of canopy closure (if not full)

These three factors adjust spatial solar radiation interception, dry matter accumulation and ultimately the spatial estimation of potato yield within a field. This depends on two factors. First, availability of the relevant information derived from the UAV imagery (see below), and second, the method by which this information is incorporated into the model. New, observed information can be incorporated into the model in several different ways. The two most common approaches are by a 'forcing' strategy or a 're-initialization or re-parameterization' strategy (Moulin et al. 1998). There are advantages and disadvantages to both of these approaches. To develop this commercial service, an approach based on both re-initialisation and re-parameterisation of the potato crop model was developed to enable the integration of spatial crop canopy cover information from UAV-mounted RGB cameras.

1) Spatial plant density information

Within the model, plant density affects the rate of canopy development and LAI. Higher densities have faster rates of canopy development. The grower at planting sets plant density, and stems per plant is a constant in the model. The assumption is therefore that the planter produces a uniform plant and stem density in the field.

Early season imagery provides an opportunity to count plants automatically as they emerge and to observe local plant densities. At very early stages of growth, new, green plants are contrasted against the soil background. Figure 12.10(a-c) shows part of a UAV image taken around emergence. This colour image is converted to greyscale and a threshold used to generate a binary image (plant or non-plant) and a count of the number of discrete elements in the threshold image. These processes are standard and common image processing techniques. The result is that for any given area the number of observed, emerged plants can be calculated and mapped (Fig. 12.10 d-e). In the first instance, this provides the grower with clear

information about emergence and establishment within the field, and possible areas for improvement. It also provides spatial information on plant density that can be entered directly into the model to improve LAI simulation.

Plant counting does have some limitations; mainly that it depends on each plant being an individual, discrete object, i.e. the plants cannot overlap. If plants do overlap, then multiple plants are considered as only one individual. Growth rates early in the season are often very fast, so there is only a short window of opportunity between emergence and the start of overlapping, a window in which imagery needs to be collected for the counting to be effective.

2) Improved estimation of emergence date

The original model calculated emergence date based on seed quality, soil temperature and planting depth. However, within a field, different areas can have different rates of crop sprouting (because of variation in soil conditions, planting depth or seed quality). Regular early season flights can provide information on emergence and the actual, or likely, date where 50% of plants have emerged. This direct approach depends on regular (1–2 day) flights around emergence. The plant counting algorithm used for plant density can be run at each time step, the maximum density found and an estimate made of the date when 50% emergence occurred. However, such high-frequency flying might be problematic, especially where regulations on UAV operation are strict, when flights cannot be fully automated, and when labour is scarce. An alternative is to take weekly early season flights to observe changes in ground cover over time and to back-predict the emergence date.

Percentage ground cover from UAV imagery can be obtained in a way similar to that of plant counts, i.e. the ratio of green to non-green pixels is the percentage ground cover in the image (Fig. 12.11). If ground cover (%) is recorded at several (usually 3+) time periods, then simple mathematical models of plant growth can be used to predict emergence. For most annual crops, canopy development follows a sigmoidal response and fitting a relevant equation allows prediction of the date when ground cover began to develop. This modelling approach has the advantage that fewer UAV flights are needed, and the timing of these flights is less critical, i.e. flights immediately pre and post-emergence are not required. Whether directly observed or modelled from early season imagery, a more accurate and spatially varying emergence date can be generated for a field.

3) Observed LAI and canopy closure date

The same information, multi-temporal ground cover (%) images during canopy development (Fig. 12.11) and the same sigmoidal canopy development model can

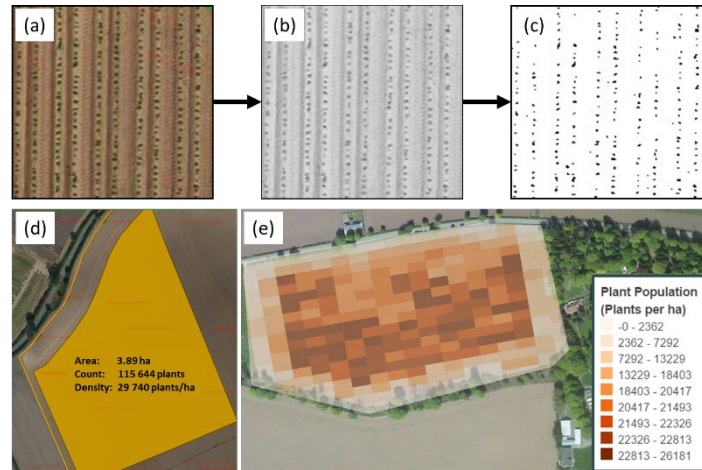


Figure 12.10: An example of a very early season high resolution image of part of a potato field ($\sim 100 \text{ m}^2$) that shows individual potato plants emerging (a). The image is converted into greyscale (b), and then a binary image using a threshold algorithm (c). The discrete elements in the binary image relate to the number of plants and can be summed for a whole field (d) or sub-field/‘pixel’ scales (e) to generate observed plant density maps.

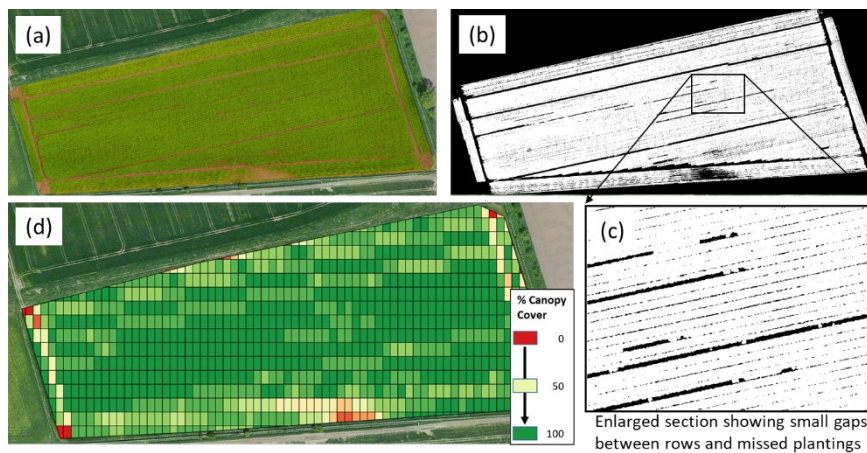


Figure 12.11: A mid-season (after expected canopy closure) UAV colour image of a potato field (a) again converted into a binary image (b) to determine % ground cover in the field. An enlarged section, illustrating missed plants and incomplete canopy fill (lower production potential) is shown (black areas) (c). Operational ‘pixels’ can be superimposed and the local canopy cover (%) calculated to form a map for spatial modelling and or management (d).

also be used to provide a forward prediction of the likely date of canopy closure as well. The estimated date of canopy closure (or full canopy development) can be verified by another UAV image around or after the expected canopy closure date. This is particularly useful in fields (or parts of fields) where local conditions restrict canopy development and canopy closure may not be achieved. Information on full canopy development (date where closure is definite or the maximum ground cover % is realised) permits the canopy development model to be updated and to reflect actual, local conditions. This provides more accurate information for potential solar radiation interception and on dry matter accumulation and yield.

Examples of improvement in model performance

To illustrate the value of incorporating the UAV imagery into the potato crop model, the model was run in several different modes in a commercial seed potato field in Scotland in 2016.

The four approaches were:

- a) the original model at the whole-field scale (using data sourced only from the grower, i.e. no UAV or in-season observations and emergence date simulated by the crop model.)
- b) the model with the emergence date adjusted (back-prediction from early-season canopy observations)
- c) the model with LAI adjusted to fit the mid-season canopy development (but retaining the original simulated emergence date from (a))
- d) the model with both emergence date and mid-season LAI adjusted according to in-season field observations

To calibrate and to validate the four approaches, 100 sites were selected in the field where manual canopy (ground cover %) and yield observations were made (see Taylor et al. 2018 for details on the sampling and data collected) and complemented with mid-season UAV flights. In this example, the emergence date and canopy information were averaged and for all cases (a–d) the model was run at the whole-field scale. Weather and soil information were constant for all four approaches. Table 12.6 shows the simulated yields for the different approaches while Fig. 12.12 shows the change in LAI within the model as the emergence date and the mid-season canopy data were included.

Table 12.6: Results from simulating potato yield using the original crop model (a) and with adjustments derived from in-season UAV imagery (b-d) to correct emergence date and LAI

Approach	Change(s) made	Observed yield (t ha ⁻¹)	Predicted yield (t ha ⁻¹)	Error (%)
a	Original model		52.23	40.67
b	Emergence date adjusted		45.26	21.90
c	LAI adjusted to mid-season observation	37.13	41.99	13.09
d	Emergence date and LAI adjusted		40.42	9.86

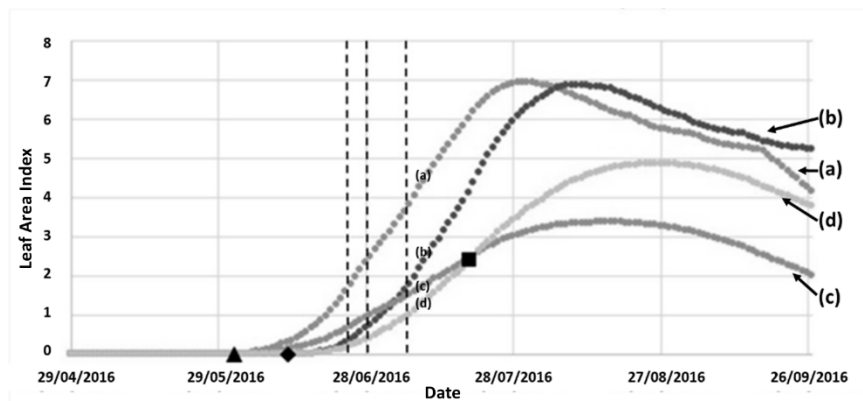


Figure 12.12: Plots of the evolution of LAI as an intermediate value within the crop model over time for the four approaches. Labels (a–d) relate to the approaches in Table 12.6. The simulated emergence date (crop model-based) is indicated by ▲, the emergence date based on early season ground cover observation (dates indicated by vertical dashed lines) is indicated by ◆ and the LAI from a UAV-derived groundcover image (July 19th) is indicated by ■.

For all four approaches, the crop model over-estimated the final yield. This might be due to the soil conditions, especially soil moisture, being incorrectly specified in the model, even though the best available data were used. The soil data were kept constant, therefore any error should be constant. The native, deterministic model approach (a) over-estimated yield by 40%. Adjusting the emergence date (b) or the mid-season LAI (c) information reduced this error to 22 and 13%, respectively. Adjusting both the emergence date and the mid-season LAI within the model reduced the error in yield prediction to <10% (3.29 t ha⁻¹). Simulating canopy development

and size correctly appears to be more important than observing emergence correctly. Plotting the daily LAI model values (Fig. 12.12) clearly illustrated the effect of incorporating in-season observations on the simulation.

The simulated emergence date (based on soil conditions and planting depth) was much earlier than expected, which led to earlier canopy development, greater dry matter accumulation and effectively a longer production season. The early season canopy observations produced an estimated emergence date 11 days later than the simulated model emergence date, resulting in a 7 t ha^{-1} reduction in yield prediction. However, canopy development was still simulated to be very strong in the field ($\text{LAI} > 5$), whereas a UAV image in mid-July revealed that full canopy closure had not occurred. When this information was included in the model, the effective LAI, dry matter accumulation and yield potential decreased, and the model output moved closer to the observed yield values.

Concluding comments

Optical sensing for crop vigour has traditionally used the response within red and near-infrared wavelengths to interpret crop vigour and biomass. This case study has shown that it is not always necessary to have these wavelengths to generate good agronomic information. The increasing availability of platforms (UAV or terrestrial) that provide high-resolution imagery, from even relatively cheap camera systems, is changing the way that optical systems are being deployed and the information used. The likelihood is that best agronomic practices will be obtained with imagery from both visible and near-infrared systems within models and decision support systems that are formulated and designed with these data sets in mind.

Concluding remarks for the Chapter

These examples illustrate that reflectance in the red and near-infrared wavelengths from the canopy of all crops provides both spatial and temporal information on the canopy condition. As agriculturists, we can link this reflectance to productivity and to crop health. However, the canopy response is generic and it is not possible to extract directly which specific biotic and or abiotic effects control the canopy response. Consequently, a wide variety of different agronomic services have been proposed using optical imagery in crop systems. However, under an assumption of good crop management (good pest and disease control) the majority have been aimed at identifying fertilizer rates. A case study on nitrogen fertilizer was not included here because this application is already widely accepted (and described elsewhere in this book). Instead, the case studies presented above to show how the use of multi-spectral optical sensing in agriculture is much broader than variable-

rate fertilizer application and is expanding, for example, to account for temporal changes over the season or to assist in high-resolution crop modelling. Multi-spectral optical sensing has been, and will continue to be, an important information source for all aspects of site-specific crop management.

However, as illustrated in these examples, it is not necessarily the type of multi-spectral sensor that is important, but the agronomic service that it is incorporated into. The sensors work; but must deliver agronomic solutions to be adopted. The same sensor, a CropCircle™, was used for both the table grape (Greece) and cotton (Brazil) case studies, but delivered different information for different services. Both cases are valid applications of the same sensor. It is also critical that any agronomic services are developed to account for any advantages (or disadvantages) associated with a particular sensing system. Even though similar sensors can be tractor-mounted or UAV-mounted, it does not follow that data from a UAV-mounted system can be incorporated directly into a decision support system built on tractor-mounted data acquisition. In a similar vein, services and decisions must be tailored to suit the local agronomy, even if the same sensing system is used. Fertilizer decisions are always linked to current crop vigour (making canopy sensing useful), however for wheat in northern Europe these decisions will be different from those for wheat in southern Europe even if the same satellite or tractor-mounted system is used because the production system needs are different.

The multispectral systems featured here are current mainstays of commercial optical sensing systems. They are affordable, robust and easy to use, but generate a generic response. Increasing the number of bands and the sensitivity (width) of the bands generates more specific information (and more expensive sensors). These sensors are termed hyperspectral (typically > 20 bands and often > 100). For optical crop sensing systems, hyperspectral sensors will eventually overtake multi-spectral systems because of the additional information that can be collected and used to separate biotic and abiotic stresses in the crop. However, these sensors are prohibitively costly at the moment for wide commercial use. Adoption is also limited by the availability of commercial services that can make use of the additional information in the hyperspectral data. Without unlocking this potential, end-users will probably continue with the cost-effective and proven multispectral systems.

Finally, optical sensing, even hyperspectral sensing, is unlikely to be the ‘holy grail’ and provide the perfect solution for all agronomic decisions. These optical sensors need to be incorporated into decision systems with other types of sensors (as illustrated in the cotton example) or with other tools (e.g. the crop models in the potato case study) to optimize production systems

References

- Acevedo-Opazo C, Tisseyre B, Guillaume S et al (2008b) The potential of high spatial resolution information to define within-vineyard zones related to vine water status. *Precis Agric* 9(5):285-302

- Acevedo-Opazo C, Tisseyre B, Ojeda H et al (2008a) Is it possible to assess the spatial variability of vine water status? *OENO One* 42(4):203-219.
- Amaral LR, Trevisan RG, Molin JP (2018) Canopy sensor placement for variable-rate nitrogen application in sugarcane fields. *Precis Agric* 19:147-160. doi:10.1007/s11119-017-9505-x
- Anastasiou E, Balafoutis A, Darra N et al (2018) Satellite and Proximal Sensing to Estimate the Yield and Quality of Table Grapes. *Agriculture* 8(7):94. doi:10.3390/agriculture8070094
- Arnall DB, Abit MJM, Taylor RK et al (2016) Development of an NDVI-based nitrogen rate calculator for cotton. *Crop Sci* 56(6):3263–3271. doi:10.2135/cropsci2016.01.0049
- Badr G, Hoogenboom G, Davenport J et al (2015) Estimating growing season length using vegetation indices based on remote sensing: A case study for vineyards in Washington state. *Trans ASABE* 58(3):551-564. doi:10.13031/trans.58.10845
- Baio FHR, Neves DC, Souza, HB et al (2018) Variable rate spraying application on cotton using an electronic flow controller. *Precis Agric*, 19(5):912–928. doi:10.1007/s11119-018-9564-7
- Baralon K, Payan, JC, Salançon E et al (2012) SPIDER: spatial extrapolation of the vine water status at the whole denomination scale from a reference site. *J Int Sci Vigne Vin* 46(3):167-175. doi:10.20870/oenone.2012.46.3.1517
- Celette F, Gary C (2013) Dynamics of water and nitrogen stress along the grapevine cycle as affected by cover cropping. *Eur J Agron* 45:142-152. doi:10.1016/j.eja.2012.10.001
- Chen H, Leinonen I, Marshall B et al (2017) Conceptual Spatial Crop Models for Potato Production *Advances in Animal Biosciences* 8(2):678–683, doi:10.1017/S2040470017000851
- Cheng G, He YN, Yue TX et al (2014) Effects of climatic conditions and soil properties on Cabernet Sauvignon berry growth and anthocyanin profiles. *Molecules* 19(9):13683-13703. doi:10.3390/molecules190913683
- Chlingaryan A, Sukkarieh S, Whelan B (2018). Machine Learning Approaches for Crop Yield Prediction and Nitrogen Status Estimation in Precision Agriculture: A Review. *Comput Electron Agr* 151:61–69. doi:10.1016/j.compag.2018.05.012
- Choné X, Van Leeuwen C, Chery PH et al (2001) Terroir influence on water status and nitrogen status of non-irrigated Cabernet Sauvignon (*Vitis vinifera*) Vegetative development, must and wine composition (example of a Medoc top estate vineyard, Saint Julien area, Bordeaux, 1997) *S Afr J of Enol Vitic* 22(1):8-15
- CONAB (2015) Acompanhamento da safra brasileira (Brazil crop production), 2(12):1–134
- Cucho-Padin, G, Loayza, H, Palacios, S. et al (2019) Development of low-cost remote sensing tools and methods for supporting smallholder agriculture. *Appl Geomatics* doi:10.1007/s12518-019-00292-5
- Dry PR, Loveys BR (1998) Factors influencing grapevine vigour and the potential for control with partial rootzone drying. *Aust J Grape Wine R* 4(3):140-148

- Feng A, Zhou J, Vories ED, Sudduth KA et al (2020). Yield Estimation in Cotton Using UAV-Based Multi-Sensor Imagery. *Biosyst Eng* 193:101–14. doi:10.1016/j.biosystemseng.2020.02.014
- Guo, W (2018) Spatial and Temporal Trends of Irrigated Cotton Yield in the Southern High Plains. *Agronomy* 8(12):298. doi:10.3390/agronomy8120298
- Hall A, Lamb DW, Holzapfel B et al (2002) Optical remote sensing applications in viticulture-a review. *Aust J Grape Wine R* 8(1):36-47
- Hall A, Wilson MA (2013) Object-based analysis of grapevine canopy relationships with winegrape composition and yield in two contrasting vineyards using multitemporal high spatial resolution optical remote sensing. *Int J Remote Sens* 34:1772–1797. doi:10.1080/01431161.2012.726753
- Henry D, Aubert H, Véronèse T (2019) Proximal Radar Sensors for Precision Viticulture. *IEEE T Geosci Remote* 57(7):4624-4635. doi:10.1109/TGRS.2019.2891886
- Horler DNH, Dockray M, Barber J (1983) The red edge of plant leaf reflectance. *Int J Remote Sens* 4(2):273-288
- Hunt Jr ER, Doraiswamy PC, McMurtrey et al (2013) A visible band index for remote sensing leaf chlorophyll content at the canopy scale. *Int J Appl Earth Obs* 21:103-112. doi:10.1016/j.jag.2012.07.020
- Iland P (2000) Techniques for chemical analysis and quality monitoring during winemaking. Patrick Iland Wine Promotions, Campbelltown, S.A, Australia
- Intrigliolo DS, Castel JR (2010) Response of grapevine cv. 'Tempranillo' to timing and amount of irrigation: water relations, vine growth, yield and berry and wine composition. *Irrigation Sci* 28(2):113. doi:10.1007/s00271-009-0164-1
- Jasper J et al (2009) Active sensing of the N status of wheat using optimized wavelength combination: impact of seed rate, variety and growth stage. In: van Henten EJ, Goense D, Lokhorst C (eds) *Precision Agriculture '09*. 7th European Conference on Precision Agriculture, Wageningen, July 2009. Wageningen Academic Publishers, Wageningen, p 23
- Johnson LF, Roczen DE, Youkhana SK et al (2003) Mapping vineyard leaf area with multispectral satellite imagery. *Comput Electron Agr* 38(1):33-44
- Kindred DR, Milne AE, Marchant B et al (2017) Spatial variation in Nitrogen requirements of cereals, and their interpretation. 303–307. *Advances in Animal Biosciences* 8(2):303-307. doi:10.1017/S2040470017001327
- Kross A, McNairn H, Lapen D et al (2015) Assessment of RapidEye vegetation indices for estimation of leaf area index and biomass in corn and soybean crops. *Int J Appl Earth Obs* 34:235-248. doi:10.1016/j.jag.2014.08.002
- Lachia N, Pichon L, Tisseyre B (2019) A collective framework to assess the adoption of precision agriculture in France: description and preliminary results after two years. In: Stafford JV (ed) *Precision Agriculture '19*. 12th European Conference on Precision Agriculture, Montpellier, 8-11 July 2013. Wageningen Academic Publishers, Wageningen, p 851
- Lamb DW, Weedon MM, Bramley RGV (2004) Using remote sensing to predict grape phenolics and colour at harvest in a Cabernet Sauvignon vineyard: Timing

- observations against vine phenology and optimising image resolution. *Aust J Grape Wine R* 10(1):46-54
- Leão TP (2016) Particle size distribution of Oxisols in Brazil. *Geoderma Regional* 7(2):216-222. doi:10.1016/j.geodrs.2016.04.003
- Leroux C, Jones H, Pichon L et al (2018) GeoFIS: An Open Source, Decision-Support Tool for Precision Agriculture Data. *Agriculture* 8(6):1-21. doi:10.3390/agriculture8060073
- Lymburner L, Beggs PJ, Jacobson CR (2000) Estimation of canopy-average surface-specific leaf area using Landsat TM data. *Photogramm Eng Rem S* 66(2):183-192
- MacKerron DKL (1985). A simple model of potato growth and yield. II. Validation and external sensitivity. *Agr Forest Meteorol* 34:285-300
- MacKerron DKL, Waister PD (1985). A simple model of potato growth and yield. I. Model development and sensitivity analysis. *Agr Forest Meteorol* 34:241-252
- MacKerron DKL, Marshall B and McNicol JW (2004) MAPP and the underlying functions that it contains. In: MacKerron DKL, Haverkort AJ (eds) *Decision support systems in potato production: bringing models to practice*. Wageningen Academic Publishers, Wageningen
- Madni A, Madni C, Lucero S et al (2019) Leveraging Digital Twin Technology in Model-Based Systems Engineering. *Systems* 7(1):7. doi:10.3390/systems7010007
- Mirasi A, Mahmoudi A, Navid H et al (2019) Evaluation of sum-NDVI values to estimate wheat grain yields using multi-temporal Landsat OLI data. *Geocarto Int* 1-16. doi:10.1080/10106049.2019.1641561
- Moulin S, Bondeau A, Delecalle R (1998) Combining agricultural crop models and satellite observations: From field to regional scales. *Int J Remote Sens*, 19(6):1021-1036. doi:10.1080/014311698215586
- Mutanga O, Skidmore, AK (2004) Narrow band vegetation indices overcome the saturation problem in biomass estimation. *Int J Remote Sens* 25:3999-4014
- Naor A, Gal Y, Bravdo B (1997) Crop load affects assimilation rate, stomatal conductance, stem water potential and water relations of field-grown Sauvignon blanc grapevines. *J Exp Bot* 48(9):1675-1680
- Oczkowski E (2016) The effect of weather on wine quality and prices: An Australian spatial analysis. *J Wine Econ* 11(1):48-65. doi:10.1017/jwe.2015.14
- OIV 2019 Statistical Report on World Vitiviniculture. International Organisation of Vine and Wine Intergovernmental Organisation. Available via <http://www.oiv.int/public/medias/6782/oiv-2019-statistical-report-on-world-vitiviniculture.pdf>. Accessed 14 Feb 2020
- Ojeda H, Andary C, Kraeva E et al (2002) Influence of pre- and postveraison water deficit on synthesis and concentration of skin phenolic compounds during berry growth of *Vitis vinifera* cv. Shiraz. *Am J Enol Viticult* 53(4):261-267
- Ollat N, Touzard JM, van Leeuwen C (2016) Climate change impacts and adaptations: New challenges for the wine industry. *J Wine Econ* 11(1):139-149. doi:10.1017/jwe.2016.3

- Portz G, Vilanova Jr NDS, Trevisan RG et al (2014) Cotton field relations of plant height to biomass accumulation and n-uptake on conventional and narrow row systems. In: Proceedings of the 12th International Conference on Precision Agriculture. Sacramento, USA, 20-23 July 2017
- QGIS Development Team. (2018) QGIS Geographic Information System, Version 3.2. <http://qgis.org> Accessed 14 Feb 2020
- R Core Team. (2018) R: A Language and Environment for Statistical Computing. Vienna, Austria. <https://www.r-project.org/> Accessed 14 Feb 2020
- Ricotta C, Avena G, De Palma A (1999) Mapping and monitoring net primary productivity with AVHRR NDVI time-series: statistical equivalence of cumulative vegetation indices. *ISPRS J Photogramm* 54(5-6):325-331
- Rodriguez D, Fitzgerald GJ, Belford R et al (2006) Detection of nitrogen deficiency in wheat from spectral reflectance indices and basic crop eco-physiological concepts. *Aust J Agr Res* 57:781-789. doi:10.1071/AR05361
- Rouse JW, Haas RH, Schell JA et al (1974) Monitoring vegetation systems in the Great Plains with ERTS. NASA special publication 351:309
- Sen F, Oksar RE, Kesgin M (2016) Effects of Shading and Covering on “Sul-tana Seedless” Grape Quality and Storability. *J Agric Sci Technol* 18:245-254
- Sharma LK, Bu H, Franzen DW et al (2016) Use of Corn Height Measured with an Acoustic Sensor Improves Yield Estimation with Ground Based Active Optical Sensors. *Comput Electron Agr* 124:254–62. doi:10.1016/j.compag.2016.04.016.
- Sibille I, Ojeda H, Prieto J et al (2007) Relation between the values of three pressure chamber modalities (midday leaf, midday stem and predawn water potential) of 4 grapevine cultivars in drought situation of the southern of France. Applications for the irrigation control. In: Proceedings of the XVth Conference of Groupe d’Etude des Systèmes de Conduite de la Vigne (GESCO). Porec, Croatia, 20-23 June 2007
- Sipiora MJ, Granda MJG (1998) Effects of pre-veraison irrigation cut-off and skin contact time on the composition, color, and phenolic content of young Cabernet Sauvignon wines in Spain. *Am J Enol Vitic* 49(2):152-162
- Spekken M et al (2013) A simple method for filtering spatial data. In: Stafford JV (ed) Precision Agriculture '13. 9th European Conference on Precision Agriculture, Lleida, July 2013. Wageningen Academic Publishers, Wageningen, p 259
- Stewart JM, Oosterhuis D, Heitholt JJ et al (eds) (2009) Physiology of cotton. Springer Science & Business Media, Dordrecht
- Sui R, Fisher DK, Reddy KN (2012) Cotton Yield Assessment Using Plant Height Mapping System. *J Agr Sci* 5(1):23–31. doi:10.5539/jas.v5n1p23
- Sun L, Gao F, Anderson MC et al (2017) Daily mapping of 30 m LAI and NDVI for grape yield prediction in California vineyards. *Remote Sens-Basel* 9(4):317. doi:10.3390/rs9040317
- Tagarakis AC, Liakos V, Fountas S et al (2013) Management zones delineation using fuzzy clustering techniques in grapevines. *Precis Agric* 14:18-39

- Tagarakis AC, Koundouras S, Fountas S et al (2018) Evaluation of the use of LIDAR laser scanner to map pruning wood in vineyards and its potential for management zones delineation. *Precis Agric* 19:334-347. doi:10.1007/s11119-017-9519-4
- Taylor JA, Acevedo-Opazo C, Ojeda H et al (2010) Identification and significance of sources of spatial variation in grapevine water status. *Aust J Grape Wine R* 16(1):218-226. doi:10.1111/j.1755-0238.2009.00066.x
- Taylor JA, Chen H, Smallwood M et al (2018) Investigations into the opportunity for spatial management of the quality and quantity of production in UK potato systems. *Field Crops Res* 229:95-102. doi:10.1016/j.fcr.2018.10.00
- Tehrani MM, Kamgar- Haghghi AA, Razzaghi, F et al (2016) Physiological and yield responses of rainfed grapevine under different supplemental irrigation regimes in Fars province, Iran. *Sci Horti-Amsterdam* 202:133-141. doi:10.1016/j.scienta.2016.02.036
- Tisseyre B, McBratney AB (2008) A technical opportunity index based on mathematical morphology for site-specific management: an application to viticulture. *Precis Agric* 9(1-2):101-113. doi:10.1007/s11119-008-9053-5
- Tisseyre B, Ojeda H, Taylor J (2007) New technologies and methodologies for site-specific viticulture. *J Int Sci Vigne Vin* 41(2):63-76. doi:10.20870/oenone.2007.41.2.852
- Trevisan R, Vilanova Jr N, Eitelwein M et al (2018) Management of Plant Growth Regulators in Cotton Using Active Crop Canopy Sensors. *Agriculture* 8(7):101. doi:10.3390/agriculture8070101
- Tsouros DC, Bibi S, Sarigiannidis PG (2019) A Review on UAV-Based Applications for Precision Agriculture. *Information* 10. doi:10.3390/info10110349
- Van Leeuwen C, Seguin G (1994) Incidences de l'alimentation en eau de la vigne, appréciée par l'état hydrique du feuillage, sur le développement de l'appareil végétatif et la maturation du raisin (*Vitis vinifera* variété Cabernet franc, Saint-Emilion, 1990). *J Int Sci Vigne Vin* 28(2):81-110
- Wang FM, Huang JF, Tang YL et al (2007) New Vegetation Index and Its Application in Estimating Leaf Area Index of Rice. *Rice Sci* 14(3):195-203. doi:10.1016/S1672-6308(07)60027-4
- Xue J, Su B (2017) Significant remote sensing vegetation indices: A review of developments and applications. *J Sensors* doi:10.1155/2017/1353691
- Zhou X, Zheng HB, Xu XQ et al (2017) Predicting grain yield in rice using multi-temporal vegetation indices from UAV-based multispectral and digital imagery. *ISPRS J Photogramm* 130:246-255. doi:10.10